Phenotypic Changes of Detrusor PDGFR Alpha Positive Cells in Spinal Cord Injury-Induced Detrusor Overactivity

Ken Lee
University of Nevada School of Medicine
Sang Park
Konkuk University School of Medicine
Pil Choi
Kangbuk Samsung Hospital, Sungkyunkwan University
Seung-Bum Ryoo
Seoul National University Hospital, Seoul National University
Haeyeong Lee
University of Nevada School of Medicine
Lauren Peri
University of Nevada School of Medicine
Tong Zhou
University of Nevada School of Medicine
Robert Corrigan
University of Nevada School of Medicine
Andrew Yanez
University of Nevada School of Medicine
Suk B Moon
Kangwon National University
Brian Perrino
University of Nevada School of Medicine
Kenton Sanders
University of Nevada School of Medicine
Sang Don Koh (skoh@medicine.nevada.edu)
University of Nevada School of Medicine

Research Article

Keywords: PDGFR, SCI, TCs, SMCs, Detrusor

DOI: https://doi.org/10.21203/rs.3.rs-505840/v1

Version of Record: A version of this preprint was published at Scientific Reports on August 11th, 2021.
See the published version at https://doi.org/10.1038/s41598-021-95781-2.

Phenotypic changes of detrusor PDGFR alpha positive cells in Spinal Cord Injury- induced Detrusor Overactivity

Ken Lee[1], Sang O Park[2], Pil C Choi[3], Seung-Bum Ryoo[4], Haeyeong Lee[1], Lauren E. Peri[1], Tong Zhou[1], Robert D. Corrigan[1], Andrew C Yanez[1], Suk B Moon[5], Brian A. Perrino[1], Kenton M. Sanders[1], Sang Don Koh[1 *]

[1]Department of Physiology and Cell Biology, University of Nevada School of Medicine, Reno, NV 89557 USA

[2]Department of Emergency Medicine, Konkuk University School of Medicine, Seoul, South Korea

[3]Department of Emergency Medicine, Kangbuk Samsung Hospital, Sungkyunkwan University, Seoul, South Korea

[4]Department of Surgery, Seoul National University Hospital, Seoul National University, Seoul, South Korea

[5]Department of Surgery, Kangwon National University, School of Medicine, Chuncheon, South Korea

***Corresponding** – Sang Don Koh, E-mail: skoh@medicine.nevada.edu,

Phone: 775-784-6908, Fax: 775-784-6903.

ABSTRACT

Volume accommodation occurs via a novel mechanism involving interstitial cells in detrusor muscles. The interstitial cells in the bladder are PDGFRα^{+}, and they restrain the excitability of smooth muscle at low levels and prevent the development of transient contractions (TCs). A common clinical manifestation of spinal cord injury (SCI)-induced bladder dysfunction is detrusor overactivity (DO). Although a myogenic origin of DO after SCI has been suggested, a mechanism for development of SCI-induced DO has not been determined. In this study we hypothesized that SCI-induced DO is related to loss of function in the regulatory mechanism provided by PDGFRα^{+} cells. Our results showed that transcriptional expression of *Pdgfra* and *Kcnn3* was decreased after SCI. Proteins encoded by these genes also decreased after SCI, and a reduction in PDGFRα^{+} cell density was also documented. Loss of PDGFRα^{+} cells was due to apoptosis. TCs in ex vivo bladders during filling increased dramatically after SCI, and this was related to the loss of regulation provided by SK channels, as we observed decreased sensitivity to apamin. These findings show that damage to the mechanism restraining muscle contraction during bladder filling that is provided by PDGFRα^{+} cells is causative in the development of DO after SCI.

.

INTRODUCTION

As the bladder fills with urine the volume increases, but during much of the filling period, intravesical pressure remains low[1]. This accommodation occurs even though there is a natural tendency for the detrusor smooth muscle cells (SMCs) to contract in response to stretch[2,3]. In fact, during bladder filling non-voiding contractions (NVCs), detected as transient increases in intraluminal pressure, occur in cystometric records from all species including human. NVCs appear to correspond to localized contractions that are also observed in ex vivo bladder preparations and have been termed as 'spontaneous phasic contractions', 'micromotions' or 'transient contractions'[4-8]. Transient contractions (TCs) increase as bladder filling proceeds[4]. Prior experiments have shown that TCs are initiated by stretch-dependent non-selective cation channels expressed by detrusor SMC[2,3]. Inward currents generated by these channels depolarize SMCs and activate L-type Ca^{2+} channels, causing generation of Ca^{2+} action potentials, Ca^{2+} entry into SMCs and contraction. Action potentials propagate to other SMCs within the same muscle bundle, but do not spread to adjacent muscle bundles.

Several studies suggest that TCs initiate afferent nerve activity and provide a major source of the sensory information conveyed to the central nervous system during bladder filling[9-12]. A recent study has clearly demonstrated the link between TCs and sensory output from bladder[4]. Increased TCs may correspond to the sensory and mechanical behaviors associated with detrussor overactivity (DO). Normal bladders have the means to restrain development of TCs, but experiments have not been sufficiently rigorous to reveal the mechanisms responsible for restraining bladder excitability and the development of TCs during filling.

We discovered a novel mechanism involving interstitial cells in detrusor muscles. Interstitial cells of the bladder were previously identified as c-Kit$^+$ cells and thought to provide excitatory input to the detrusor[13,14], but more recent immunohistochemical evaluation showed few c-Kit$^+$ cells, other than mast cells, in the bladder of several species[15]. In fact, the interstitial cells in the bladder are PDGFRα$^+$, and they provide inhibitory regulation of detrusor muscles[16-20]. Inhibitory regulation is enhanced by purines and by stretch, making it an ideal mechanism for regulating detrusor excitability and restraining TCs during bladder filling. Rigorous confirmation of the hypothesis that inhibitory regulation during bladder filling is provided by PDGFRα$^+$ cells would be to demonstrate that pathological conditions in which DO develops are associated with loss or remodeling of PDGFRα$^+$ cells. Therefore, we evaluated the status of PDGFRα$^+$ cells in spinal cord injury (SCI) animal models that are known to develop DO.

Clinical manifestations of SCI-induced bladder dysfunction involve a combination of storage and voiding problems. A myogenic origin of DO after SCI has also been suggested due to abnormal muscle reactivity ("the myogenic hypothesis")[21] without studying precise mechanisms for DO after SCI. Since obtaining human whole bladder due to SCI is extremely difficult, we investigated the mechanisms of DO in the acute phase of SCI using murine model.

RESULTS

1. Changes in transcriptional expression of SCI-induced detrusor muscles

We harvested detrusor muscles from control (sham) mice and 1, 2, 3, 7, 14 and 30 days after SCI. *Pdgfra and Kcnn3* expression were decreased in detrusor muscles 24 hr after SCI. Reduced *Pdgfrα* and *Kcnn3* expression persisted for at least 1 month after SCI (n=4, Fig. 1A & B). *Pdgfra* and *Kcnn3* expression also decreased in sorted PDGFRα^+ cells 7days after SCI, as compared with sorted PDGFRα^+ cells from sham mice (n=4, Fig. 1C). We also isolated and sorted SMCs from smMHC/eGFP mice. Expression of *Myh11* (SM myosin heavy chain), *Kcnma1* (BK α_{slo}) and *Cacna1C* (Cav1.2) were unchanged in SMCs after SCI (n=4, Fig. 1D).

2. Changes in protein expression in SCI-induced detrusor muscles

Three approaches were used to characterize changes in protein expression. Firstly, immunohistochemistry was used to examine the expression and distribution of PDGFRα and SK3 immunoreacitvity in SCI. PDFGRα and SK3-like immunoreactivity decreased in detrusor muscles after SCI in a time dependent manner (Fig. 2). We also used PDFGRα/eGFP mice to examine the density of green nuclei in control and SCI. The density of eGFP were decreased in SCI (3 day and 7day) compared to control. Since SCI can show bladder distension, we normalized the eGFP expression by calculated the surface area (e.g. 63 mm^2 in control vs 111 mm^2 in SCI, n=3, respectively). PDGFRα$^+$ cells also decreased to 53% (3 day) and 35% (7 day) after SCI in PDGFRα/eGFP mice, (Fig. 3A-C). We confirmed these findings by Western analysis and verified reduction in PDGFRα protein in detrusor muscles of SCI mice (n= 4, Fig. 3D & E). These findings were

consistent with the transcriptional changes observed after SCI (see Fig. 1), and suggest overall reduction in PDGFRα⁺ cells and reduced expression of SK3 that would negatively impact the regulation of excitability provided by PDGFRα⁺ cells in the bladder.

3. Apoptosis of PDGFRα^+ cells in SCI

We examined changes in the expression of apoptosis pathways to better understand the fate of PDGFRα⁺ cells after SCI. RNA-seq of whole muscle samples showed geneset scores computed for the apoptosis-related KEGG and GOBP terms, respectively, using the FAIME algorithm[22]. The apoptosis-related geneset score was significantly increased (t-test: P <0.05) in detrusor muscles after SCI (Fig. 4A). Apoptosis-related genes, including *Apaf1, Capns1, and Casp3*, were significantly upregulated (FC>1.5 and *FDR* <0.05) in detrusor muscles 3 days after SCI (Fig. 4B). Time dependent increases in expression of *Apaf1* (Fig. 4C) and *Caspase3* (Fig, 4D) in detrusor muscles after SCI (as compared to sham; n=4 for each period) were confirmed by qPCR.

4. Ex vivo preparation to confirm the role of PDGFRα^+ cells in SCI

Ex vivo bladder preparations were used to characterize the relationship between intravesical volumes and pressures in bladders after SCI. Pressure-volume studies done ex vivo exclude extrinsic neural reflexes during filling. SK channels are highly expressed in detrusor PDGFRα⁺ cells, and antagonists of these channels increase TCs during filling[17]. We examined the effects of the SK channel antagonist, Apamin (300nM) on bladders from control and SCI (up to 1 month).

In sham preparations, infusion of Krebs–Ringer bicarbonate (20 µl/min) generated repeatable responses consisting of small amplitude, low frequency of TCs (Fig. 5A).

Apamin (300 nM added to the bathing solution) increased the amplitude (6.9±1.2 cmH_2O, $P<0.01$) and frequency (65±12 events, $P<0.01$, $n=11$) of TCs during bladder filling, as compared to control (2.1±0.5 cmH_2O in amplitude and 22±9.1 events in frequency; Fig. 5A, Table 1). At 1, 3, 7, 14 and 30 days after SCI, the amplitude and frequency of TCs during filling were increased (Fig. 5B-F, Table 1). Enhanced TCs during filling persisted for at least 30 days after SCI, and apamin failed to induce significant changes of amplitude (from 7 days) and frequency (from 1 day) of TCs after SCI (Fig. 5B-F, Table 1) indicating that development of DO after SCI progressed for up to 1 month after SCI. Bladder capacity and filling time to reach 30cmH_2O were also increased in all of SCI groups compared to sham (Table 2). The enlarged bladder capacity due to lack of voluntary voiding and prolonged infusion time was prominent in 30 days.

DISCUSSION

In this study we investigated responses of the murine bladder and the status of PDGFRα$^+$ cells after SCI. PDGFRα$^+$ cells and the functions provided by these cells in regulating bladder contractions during filling were greatly decreased after SCI. TCs increased dramatically during bladder filling, and accompanying this change in function, *Pdgfra* and *Kcnn3* expression decreased. Expression of PDGFRα and SK3 protein also decreased. Detrusor muscles displayed apoptotic loss of PDGFRα$^+$ cells. The increase in TCs was due to decreased sensitivity to apamin during bladder filling, which is consistent with the reduction in expression of SK3 and loss of PDGFRα$^+$ cells that express SK3 channels. These findings demonstrate a novel mechanism for development of DO after SCI that is linked to loss of the inhibitory regulation provided by PDGFRα$^+$ cells during bladder filling.

PDGFRα$^+$ cells regulate detrusor excitability during bladder filling[23]. SK channel antagonists potentiate the amplitude of spontaneous contractions in murine[24], guinea pig[25] and human[26] detrusor muscles. The effects of apamin are likely due to blocking SK channels in PDGFRα$^+$ cells which have a high expression of SK3 channels, because the current density from SK channels is minimal in SMCs and not even resolvable in murine SMCs at physiological potentials[27]. Thus, PDGFRα$^+$ cells express a powerful mechanism to suppress excitability and allow the bladder to fill with minimal activation of TCs and sensory discharge[23]. Downregulation of *Pdgfra* and *Kcnn3* genes can lead to the development of DO after SCI. Indeed, transcriptional analysis revealed downregulation of *Pdgfra* and *Kcnn3* in early stage of SCI bladder.

IHC showed that the distribution of PDGFRα$^+$ cells decreases in detrusor muscles after SCI. The immunohistochemistry findings were confirmed using a reporter strain of mice with expression of eGFP in nuclei of PDGFRα$^+$ cells, as a relatively low density of eGFP$^+$ cells was found in bladders of PDGFRα/eGFP mice after SCI. However, IHC is not reliable method to quantify loss of protein, so protein expression in extracts of detrusor muscles was measured by Western analyses. Western blots showed the downregulation of PDGFRα expression and SK3 expression which was mirrored by transcriptional expression.

Loss of PDGFRα$^+$ cells caused by SCI were due to apoptotic changes in detrusor PDGFRα$^+$ cells although the mechanism inducing apoptosis in detrusor PDGFRα$^+$ cells by SCI has not been elucidated. *Apaf1* as well as *caspase3* had a trend to be increased after SCI compare to sham indicating that cell death occurred as a result of SCI. We speculate that apoptosis of PDGFRα$^+$ cells may be caused by the reduced expression and function of neurotropins[28,29]. The mechanism causing damage to the regulatory function provided by PDGFRα$^+$ cells after SCI is an important topic for future research.

Ex vivo preparations were used in the present study to isolate bladders and exclude connections from central and spinal reflexes. Release of mediators from the urothelium may also influence detrusor excitability, but substances and receptors involved in such a mechanism have not been identified. Ex vivo bladder developed increased TCs after SCI as compared to sham bladders (see Table 1), and enhanced TCs persisted for at least 30 days after SCI. Effects of apamin on responses to bladder filling remained for up to 72 hr after SCI, but the sensitivity to apamin decreased after SCI due to partial loss

of PDGFRα^{+} cells and downregulation of SK3 channels. These findings present in ex vivo bladders suggest that myogenic mechanisms are sufficient to generate DO.

SCI patients have less opportunity to see a urologist due to other complications that often need to be treated ahead of bladder dysfunction. This prevents patients from early and appropriate examination and treatment of lower urinary tract dysfunction in the early phase of SCI. Although there are many reports of DO after recovery from spinal shock[30-35], only a few reports confirm development of DO in the acute phase of SCI (i.e. 3 – 40 days after SCI)[36,37]. Early treatment to avoid higher intravesical pressure with lower bladder compliance followed by vesicoureteral reflux associated with DO has been suggested to keep patients' renal and bladder function serving as a 'low pressure tank' without waiting for the irreversible complications of SCI[36,37]. Given the importance of an early intervention for a treatment especially focusing on a myogenic aspect, preventing the phenotypic change of PDGFRα^{+} cells and rescuing the function of SK channels in bladder PDGFRα^{+} cells might be a promising target to avoid development of DO after SCI.

METHODS

Spinal cord injury (SCI) animal model

All experimental procedures were conducted in accordance with the National Institutes of Health *Guide for the Care and Use of Laboratory Animals* and the animal use protocol, reviewed and approved by the Institutional Animal Use and Care Committee at the University of Nevada. C57BL/6 (male mice, 8-12 wks old), *Pdgfra*$^{tm11(EGFP)Sor}$/J (PDGFRα/eGFP, Jackson lab) and smMHC/Cre/eGFP (SMC/eGFP) from Jackson Lab used for SCI operations and age-matched control. Laminectomies were performed under isoflurane anesthesia (3 - 4 % with a balance of oxygen for induction followed by 2 % for maintenance), and the spinal cord (T11-T13) were exposed without any damage or compression to the surrounding dura. Dumont #5 forceps were positioned in the middle of the exposed spinal cord segment to perform complete spinal cord transection. Complete spinal cord transection was done at T12 confirmed by retraction of rostal and caudal cut ends of spinal cord under surgical microscope, which had a space approximately at 2 mm. Control animals received sham operations with exposing the vertebrae at same level as SCI without damaging any spinal cord and dura. Enrofloxacin (5 mg/kg) was applied subcutaneously for three days after SCI followed by twice a week after SCI surgery until ex vivo or molecular evaluation was done. The bladder was manually squeezed to eliminate the residual urine of bladder once daily. Bladders were collected for experiments at 1, 3, 7, 14 and 30 days after SCI surgery and in sham control.

Ex vivo preparation

Bladders were removed. A PE50 catheter (Intramedic, Fisher Scientific, Santa Clara, CA)

with a cuff was placed in the urethral opening and ligated tightly with silk thread just above the ureterovesical junction and constant monitoring of pressure. Intravesical pressure were recorded with reference to atmospheric pressure (p = 0) at the level of the bladder connected to a quad-bridge amplifier (AD Instruments) interfaced to a computer. Krebs–Ringer bicarbonate solution (37°C) was infused (25 µl/min) and stopped when bladder pressures reach 30-40 cm/H_2O to avoid a permanent damage[4]. At least 3 fills will be performed under each experimental condition to ensure reproducibility. The effect of apamin was tested on sham and spinal cord injured bladder. Ex vivo data were captured using the threshold search by Clampfit 10 (Molecular Device) with baseline adjustment to examine the frequency and amplitude of transient contractions occurring during the filling phase.

Molecular preparation

Dissection of detrusor smooth muscles and RNA isolation in sham and SCI were identical as previously described[18]. For quantitative analysis of transcripts, PDGFRα$^+$ cells and SMC/eGFP were purified by fluorescence-activated cell sorting and detrusor muscles for molecular tests. Total RNA was isolated from detrusor muscles, PDGFRα$^+$ cells and SMC/eGFP using illustra RNAspin Mini RNA Isolation kit (GE Healthcare, Little Chalfont, UK), and first-strand cDNA was synthesized using SuperScript III (Invitrogen, Carlsbad, CA, USA), according to the manufacturer's instructions. PCR was performed with specific primers using Go-Taq Green Master Mix (Promega Corp., Madison, WI, USA). The following PCR primers designed against murine sequences were used (GenBank accession number is given in parentheses for the reference nucleotide

sequence used): *Pdgfra* (NM_011058) and *Kcnn3* (NM_080466). Quantitative PCR (qPCR) was performed with the same primers as PCR using Fast SYBR Green chemistry (Applied Biosystems, Foster City, CA, USA) on the 7900HT Real Time PCR System (Applied Biosystems). Regression analysis of the mean values of three multiplex qPCRs for the $\log_{10}$-diluted cDNA was used to generate standard curves. Unknown amounts of messenger RNA (mRNA) were plotted relative to the standard curve for each set of primers and graphically plotted using Microsoft Excel. This gave transcriptional quantification of each gene relative to the endogenous glyceraldehyde 3-phosphate dehydrogenase (*Gapdh*) standard after log transformation of the corresponding raw data.

Transcriptomes profiled by mRNA-seq (Novogene Co Ltd) were investigated to identify the genes and pathways potentially involved in the regulation of excitability in PDGFRα$^+$ cells upon SCI treatment. Total RNA was obtained from detrusor muscles in sham and SCI. Using the SAM tool[38], the genes with false discovery rate (FDR) < 5% and fold change (FC) > 1.5% were deemed to be differentially expressed. The *FAIME* algorithm[22] was applied to assign gene expression-based geneset scores for the “apoptosis” related genes defined by both the Kyoto Encyclopedia of Genes and Genomes (KEGG)[39] and Gene Ontology (GO)[40] databases. The *FAIME* method generates geneset scores using the rank-weighted gene expression of individual samples, which determines whether an a priori defined set of genes shows statistically significant, concordant expression differences between two biological states (e.g. sham vs. SCI), and provides a mechanistic interpretation of the deregulated genes.

Whole mount immunohistochemistry

C57BL/6 and *Pdgfra*$^{tm11(EGFP)Sor}$/J bladders were cut open from the neck up to the dome. Tissues were dissected in Krebs ringer solution containing 118.5 mM NaCl, 4.7 mM KCl, 2.5 mM $CaCl_2$, 1.2 mM $MgCl_2$, 23.8 mM $NaHCO_3$, 1.2 mM KH_2PO4 and 11 mM dextrose, then pinned down on Sylgard dish and stretched 150% from the resting state. For urothelial denudation, urothelium was removed and surface of the muscle was scraped to remove any residual sub-urothelial cells. Fixation and incubation of tissues were identical as previously described[16]. For double labelling studies, tissues were re-blocked for 1 hr in 10% normal donkey serum (Sigma-Aldrich) and incubated overnight in antibody of choice, diluted in 0.5% Triton-X (Sigma-Aldrich) and incubated in the appropriate Alexa Fluor (Invitrogen) antibody diluted 1:1000 in PBS for 1 hr. Processed tissues were mounted with Aqua mount mounting media (Lerner Laboratories, Pittsburgh, PA, USA) on glass slides and cover slipped and imaged. The primary antibodies of PDGFRα (R&D Systems, Inc.) and SK3 (Alamone Labs) were used and primary antibodies were omitted in the procedure for negative controls.

Automated Capillary Electrophoresis and Chemiluminescent Western Blotting

Muscles were snap-frozen in liquid N_2, and stored at −80°C. For analysis, the methods for homogenization, centrifugation and collection of the supernatants were identical as previously reported[41,42]. Protein concentrations were determined by Bradford assay[42]. Analysis of protein expression was performed according to the User Guide using a ProteinSimple Wes instrument (CA, USA). Each sample was mixed with fluorescent 5x Master Mix, incubated at 95°C for 5 min and then loaded into a Wes 12–230 kDa prefilled

plate, along with a biotinylated protein ladder, blocking buffer, primary antibodies, ProteinSimple HRP-conjugated anti-rabbit secondary antibody, luminol peroxide, and washing buffer. The plates and capillary cartridges were placed into the Wes for electrophoresis and chemiluminescence immunodetection by a CCD camera using default settings. Compass software was used to acquire and analyze the data and generate gel images and chemiluminescence intensities. Protein expression levels are expressed as the chemiluminescence intensity area under the primary antibody peak per µg protein.

Drugs

All reagents were purchased from Sigma-Aldrich (St Louis, MO, USA) and apamin (Tocris, UK) solubilized in the bath solution for ex vivo recordings.

Statistical analyses

All data are expressed as means ± SEM. “n” represents the number of experiments. All statistical analyses were performed using GraphPad Prism. A paired and unpaired Student's *t* test was used to compare groups of data and differences were considered to be significant at $P < 0.05$. This study was carried out in compliance with the ARRIVE guidelines.

Funding: This research was supported by the NIH/NIDDK R01 DK098388 for SDK.

Author Information:
Affiliations
Department of Physiology and Cell Biology, University of Nevada School of Medicine, Reno, NV 89557 USA
Ken Lee, Haeyeong Lee, Lauren E. Peri, Tong Zhou, Robert D. Corrigan, Andrew C Yanez, Brian A. Perrino, Kenton M. Sanders & Sang Don Koh

Department of Emergency Medicine, Konkuk University School of Medicine, Seoul, South Korea
Sang O Park

Department of Emergency Medicine, Kangbuk Samsung Hospital, Sungkyunkwan University, Seoul, South Korea
Pil C Choi

Department of Surgery, Seoul National University Hospital, Seoul National University, Seoul, South Korea
Seung-Bum Ryoo

Department of Surgery, Kangwon National University, School of Medicine, Chuncheon, South Korea
Suk B Moon

Authors' contributions: SOP, PCC, S-BR, SBM and HL performed spinal cord surgery. Ex vivo data were collected and analyzed by SOP, PCC, S-BR, RDC, ACY, SBM and HL. HL and LEP performed cell sorting and molecular study. TZ analyzed RNA-seq data. Immunohistochemistry were performed by ACY and SBM and WES were performed by BAP. KMS and SDK shared in the design of experiments, interpretation of the data and the writing of the manuscript. All authors approved the final version of the manuscript.

Competing interests: No conflict of interest

References

1 Wein, A. J. Normal and abnormal function: An overview, Bladder Dysfunction in the Adult: The basis for Clinical Management, Current Clinical Urology. Springer Science+Business Media New Yoork. p. 19-22. (2014)

2 Wellner, M. C. & Isenberg, G. Properties of stretch-activated channels in myocytes from the guinea-pig urinary bladder. *J Physiol* **466**, 213-227 (1993).

3 Wellner, M. C. & Isenberg, G. Stretch effects on whole-cell currents of guinea-pig urinary bladder myocytes. *J Physiol* **480 (Pt 3)**, 439-448 (1994).

4 Heppner, T. J., Tykocki, N. R., Hill-Eubanks, D. & Nelson, M. T. Transient contractions of urinary bladder smooth muscle are drivers of afferent nerve activity during filling. *J Gen Physiol* **147**, 323-335, doi:10.1085/jgp.201511550 (2016).

5 Drake, M. J. *et al.* Partial outlet obstruction enhances modular autonomous activity in the isolated rat bladder. *J Urol* **170**, 276-279, doi:10.1097/01.ju.0000069722.35137.e0 (2003).

6 Gillespie, J. I. Phosphodiesterase-linked inhibition of nonmicturition activity in the isolated bladder. *BJU Int* **93**, 1325-1332, doi:10.1111/j.1464-410X.2004.04840.x (2004).

7 Parsons, B. A., Drake, M. J., Gammie, A., Fry, C. H. & Vahabi, B. The validation of a functional, isolated pig bladder model for physiological experimentation. *Front Pharmacol* **3**, 52, doi:10.3389/fphar.2012.00052 (2012).

8 Vahabi, B. & Drake, M. J. Physiological and pathophysiological implications of micromotion activity in urinary bladder function. *Acta Physiol (Oxf)* **213**, 360-370, doi:10.1111/apha.12373 (2015).

9 Iijima, K., Igawa, Y., Wyndaele, J. J. & De Wachter, S. Mechanosensitive primary bladder afferent activity in rats with and without spinal cord transection. *J Urol* **182**, 2504-2510, doi:10.1016/j.juro.2009.07.012 (2009).

10 Kanai, A. & Andersson, K. E. Bladder afferent signaling: recent findings. *J Urol* **183**, 1288-1295, doi:10.1016/j.juro.2009.12.060 (2010).

11 Satchell, P. & Vaughan, C. Efferent pelvic nerve activity, ganglionic filtering, and the feline bladder. *Am J Physiol* **256**, R1269-1273 (1989).

12 Yu, Y. & de Groat, W. C. Sensitization of pelvic afferent nerves in the in vitro rat urinary bladder-pelvic nerve preparation by purinergic agonists and cyclophosphamide pretreatment. *Am J Physiol Renal Physiol* **294**, F1146-1156, doi:10.1152/ajprenal.00592.2007 (2008).

13 McCloskey, K. D. *et al.* Comparison of mechanical and electrical activity and interstitial cells of Cajal in urinary bladders from wild-type and W/Wv mice. *Br J Pharmacol* **156**, 273-283, doi:10.1111/j.1476-5381.2008.00006.x (2009).

14 McCloskey, K. D. & Gurney, A. M. Kit positive cells in the guinea pig bladder. *J Urol* **168**, 832-836 (2002).

15 Gevaert, T. *et al.* The stem cell growth factor receptor KIT is not expressed on interstitial cells in bladder. *J Cell Mol Med* **21**, 1206-1216, doi:10.1111/jcmm.13054 (2017).

16 Koh, B. H. *et al.* Platelet-derived growth factor receptor-alpha cells in mouse urinary bladder: a new class of interstitial cells. *J Cell Mol Med* **16**, 691-700, doi:10.1111/j.1582-4934.2011.01506.x (2012).
17 Lee, H. *et al.* Premature contractions of the bladder are suppressed by interactions between TRPV4 and SK3 channels in murine detrusor PDGFRalpha+ cells. *Sci Rep* **7**, 12245, doi:10.1038/s41598-017-12561-7 (2017).
18 Lee, H., Koh, B. H., Peri, L. E., Sanders, K. M. & Koh, S. D. Functional expression of SK channels in murine detrusor PDGFR+ cells. *J Physiol* **591**, 503-513, doi:10.1113/jphysiol.2012.241505 (2013).
19 Lee, H., Koh, B. H., Peri, L. E., Sanders, K. M. & Koh, S. D. Purinergic inhibitory regulation of murine detrusor muscles mediated by PDGFRalpha+ interstitial cells. *J Physiol* **592**, 1283-1293, doi:10.1113/jphysiol.2013.267989 (2014).
20 Lee, H. *et al.* UTP activates small-conductance Ca2+-activated K+ channels in murine detrusor PDGFRalpha+ cells. *Am J Physiol Renal Physiol* **309**, F569-574, doi:10.1152/ajprenal.00156.2015 (2015).
21 Brading, A. F. & Turner, W. H. The unstable bladder: towards a common mechanism. *Br J Urol* **73**, 3-8 (1994).
22 Yang, X. *et al.* Single sample expression-anchored mechanisms predict survival in head and neck cancer. *PLoS Comput Biol* **8**, e1002350, doi:10.1371/journal.pcbi.1002350 (2012).
23 Koh, S. D., Lee, H., Ward, S. M. & Sanders, K. M. The Mystery of the Interstitial Cells in the Urinary Bladder. *Annu Rev Pharmacol Toxicol*, doi:10.1146/annurev-pharmtox-010617-052615 (2017).
24 Thorneloe, K. S. *et al.* Small-conductance, Ca(2+) -activated K+ channel 2 is the key functional component of SK channels in mouse urinary bladder. *Am J Physiol Regul Integr Comp Physiol* **294**, R1737-1743, doi:10.1152/ajpregu.00840.2006 (2008).
25 Parajuli, S. P., Soder, R. P., Hristov, K. L. & Petkov, G. V. Pharmacological activation of small conductance calcium-activated potassium channels with naphtho[1,2-d]thiazol-2-ylamine decreases guinea pig detrusor smooth muscle excitability and contractility. *J Pharmacol Exp Ther* **340**, 114-123, doi:10.1124/jpet.111.186213 (2012).
26 Afeli, S. A., Rovner, E. S. & Petkov, G. V. SK but not IK channels regulate human detrusor smooth muscle spontaneous and nerve-evoked contractions. *Am J Physiol Renal Physiol* **303**, F559-568, doi:10.1152/ajprenal.00615.2011 (2012).
27 Herrera, G. M. *et al.* Urinary bladder instability induced by selective suppression of the murine small conductance calcium-activated potassium (SK3) channel. *J Physiol* **551**, 893-903, doi:10.1113/jphysiol.2003.045914 (2003).
28 McEvilly, R. J. *et al.* Requirement for Brn-3.0 in differentiation and survival of sensory and motor neurons. *Nature* **384**, 574-577, doi:10.1038/384574a0 (1996).
29 Yoon, S. O., Casaccia-Bonnefil, P., Carter, B. & Chao, M. V. Competitive signaling between TrkA and p75 nerve growth factor receptors determines cell survival. *J Neurosci* **18**, 3273-3281 (1998).
30 de Groat, W. C. A neurologic basis for the overactive bladder. *Urology* **50**, 36-52; discussion 53-36 (1997).

31 Choudhary, M., van Asselt, E., van Mastrigt, R. & Clavica, F. Neurophysiological modeling of bladder afferent activity in the rat overactive bladder model. *J Physiol Sci* **65**, 329-338, doi:10.1007/s12576-015-0370-y (2015).
32 Coelho, A., Oliveira, R., Cruz, F. & Cruz, C. D. Impairment of sensory afferents by intrathecal administration of botulinum toxin A improves neurogenic detrusor overactivity in chronic spinal cord injured rats. *Exp Neurol* **285**, 159-166, doi:10.1016/j.expneurol.2016.05.029 (2016).
33 Dorsher, P. T. & McIntosh, P. M. Neurogenic bladder. *Adv Urol* **2012**, 816274, doi:10.1155/2012/816274 (2012).
34 Miyazato, M., Yoshimura, N. & Chancellor, M. B. The other bladder syndrome: underactive bladder. *Rev Urol* **15**, 11-22 (2013).
35 Taweel, W. A. & Seyam, R. Neurogenic bladder in spinal cord injury patients. *Res Rep Urol* **7**, 85-99, doi:10.2147/RRU.S29644 (2015).
36 Bywater, M., Tornic, J., Mehnert, U. & Kessler, T. M. Detrusor Acontractility after Acute Spinal Cord Injury-Myth or Reality? *J Urol* **199**, 1565-1570, doi:10.1016/j.juro.2018.01.046 (2018).
37 Watanabe, T. *et al.* High incidence of occult neurogenic bladder dysfunction in neurologically intact patients with thoracolumbar spinal injuries. *J Urol* **159**, 965-968 (1998).
38 Tusher, V. G., Tibshirani, R. & Chu, G. Significance analysis of microarrays applied to the ionizing radiation response. *Proc Natl Acad Sci U S A* **98**, 5116-5121, doi:10.1073/pnas.091062498 (2001).
39 Kanehisa, M. & Goto, S. KEGG: kyoto encyclopedia of genes and genomes. *Nucleic Acids Res* **28**, 27-30, doi:10.1093/nar/28.1.27 (2000).
40 Ashburner, M. *et al.* Gene ontology: tool for the unification of biology. The Gene Ontology Consortium. *Nat Genet* **25**, 25-29, doi:10.1038/75556 (2000).
41 Dudem, S. *et al.* LINGO1 is a regulatory subunit of large conductance, Ca(2+)-activated potassium channels. *Proc Natl Acad Sci U S A* **117**, 2194-2200, doi:10.1073/pnas.1916715117 (2020).
42 Li, W., Sasse, K. C., Bayguinov, Y., Ward, S. M. & Perrino, B. A. Contractile Protein Expression and Phosphorylation and Contractility of Gastric Smooth Muscles from Obese Patients and Patients with Obesity and Diabetes. *J Diabetes Res* **2018**, 8743874, doi:10.1155/2018/8743874 (2018).

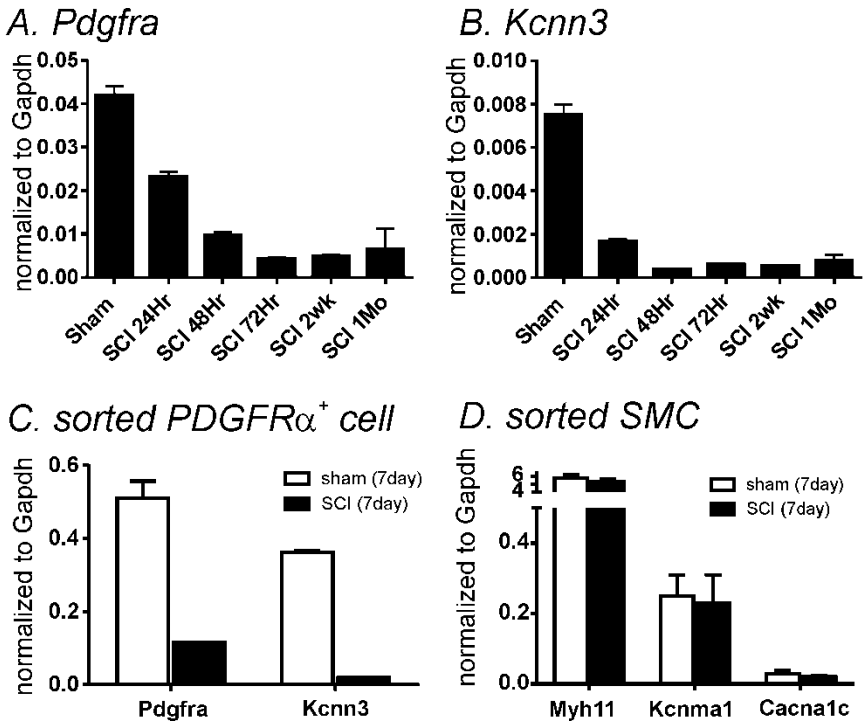

Figure 1. Quantitative analysis of transcripts in Sham and after SCI. ***A&B.*** *Pdgfra* and *Kcnn3* transcripts are decreased up to 1month after SCI in detrusor muscles. ***C***. Transcripts of *Pdgfra* and *Kcnn3* from sorted PDGFRα^{+} cells in SCI (7day) decreased compared to sham (7day). ***D.*** Transcripts including *Myh11, Kcnma1* and *Cacna1C* from sorted SMCs showed no significant change in SCI (7day). Error bars denote standard deviation from n=4.

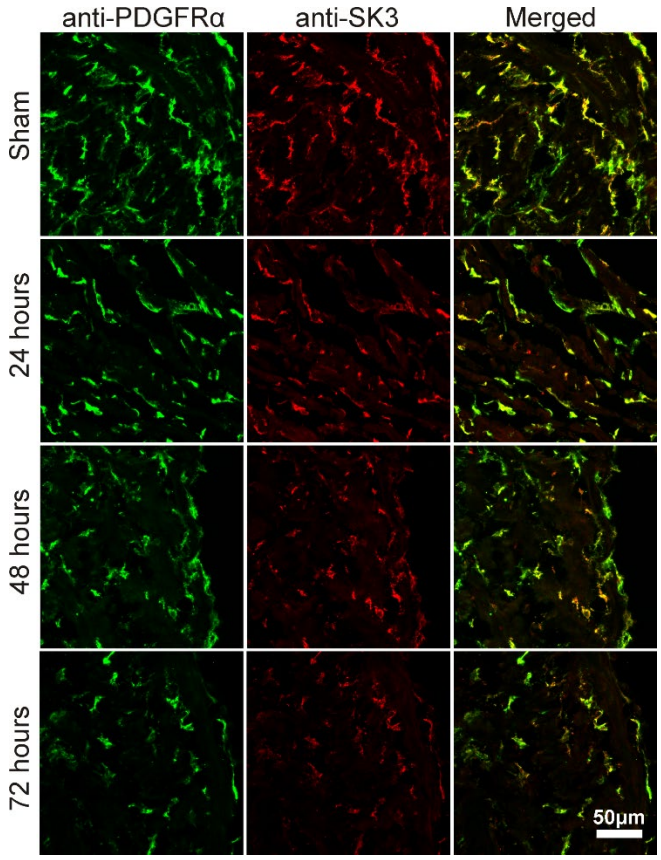

Figure 2. PDGFRα immunoreactivity of detrusor muscle layer in control and SCI. **I**mmunoreactivity of PDGFRα (green) and SK3 (red) in control (sham). SCI (24hr, 48hr and 72 hr).

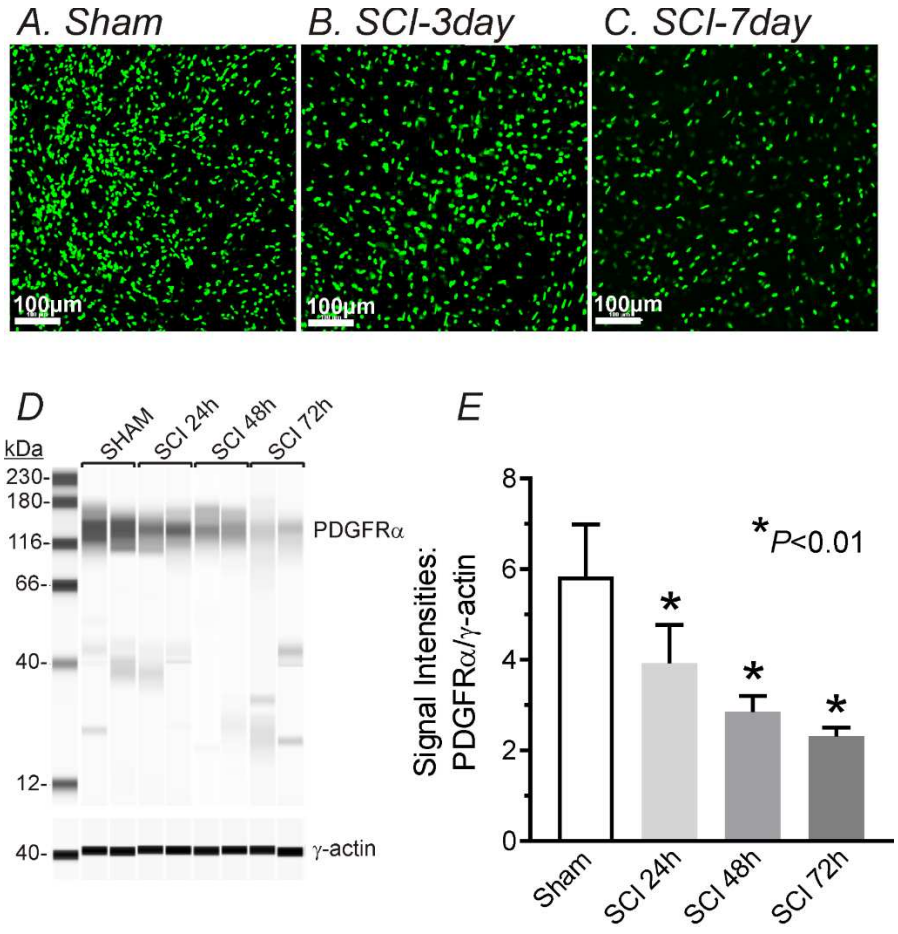

Fig. 3. Density of PDFGRα/eGFP cells and Microcapillary electrophoresis and immunodetection of PDGFRα by WES in control and SCI detrusor muscles. ***A-C.*** Far fewer eGFP^{+} nuclei (reporter for PDGFRα^{+} cells) were found in detrusor muscles after SCI. ***D.*** Representative Wes full length gel image of PDGFRα expression in murine detrusor muscles following SCI. 100,000 x g pellet, 1μg/lane, γ-action was used for normalization. ***E.*** Normalized signal intensities of PDGFRα by g-actin following SCI periods.

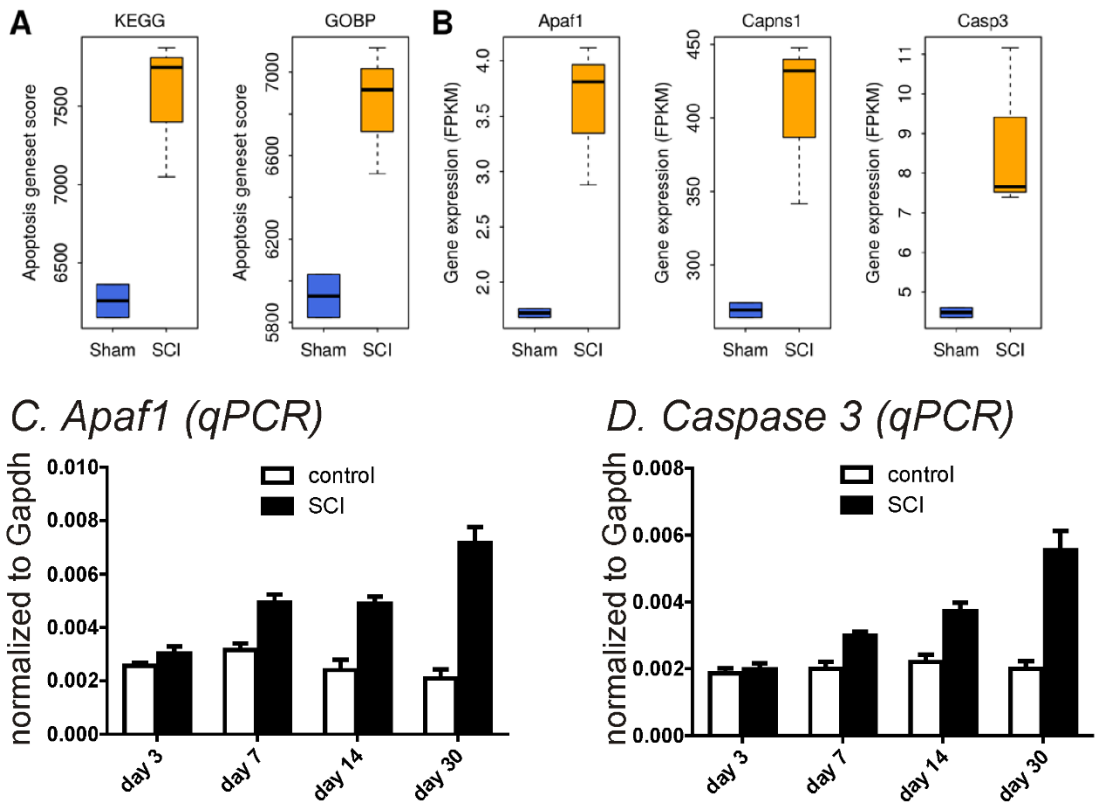

Fig. 4. SCI -induced alteration in apoptosis-related genes by RNA-seq (A &B) and qPCR (C & D). ***A***. Apoptosis geneset scores upregulated in SCI for both the KEGG and GOBP definitions. ***B.*** Expression of three apoptosis-related genes were upregulated in SCI. ***C*** *&* *D.* qPCR from sorted PDGFRα⁺ cells in SCI up to 30days showed an increase in apoptosis-related transcripts (*Apaf1* in **C** and *Caspase3* in **D**).

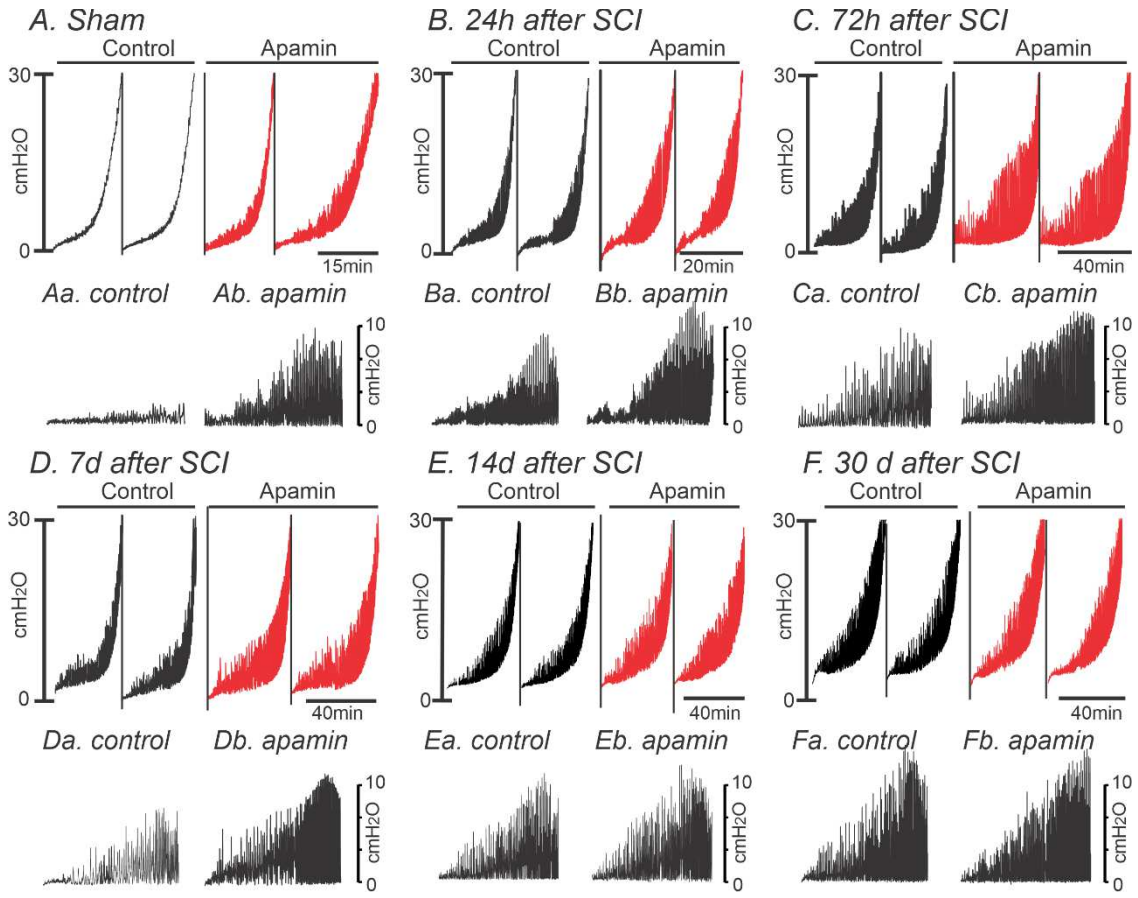

Figure 5: The effects of apamin on transient contractions (TCs) of sham, 1,3,7,14 and 30day after SCI using *ex vivo* preparation. ***A-F.*** *Ex vivo* pressure-response curve for control and apamin application. ***Aa,b-Fa,b***. Expanded time scales with adjustment of baseline under control (***a***) and apamin (***b***) from above panels.

Table 1. Summarized data of frequency and amplitude before and after apamin.

	Peak Amplitude (cmH_2O)		Frequency (events per min)	
	control	apamin	control	apamin
Sham (n=11)	2.1±0.5	6.9±1.2#	22±9.1	65±12.0#
1day (n=10)	4.8±1.2*	7.2±1.5#	52±9.7*	71±13.4
2day (n=12)	5.1±0.6*	7.8±1.1#	56±11.1*	69±11.7
3day (n=9)	5.9±1.2*	7.2±1.4	55±10.8*	64±9.2
14day (n=6)	7.0±1.3*	8.3±2.3	67±10.4*	69±11.6
30day (n=6)	6.6±0.7*	6.9±0.5	96±6.7*	98±4.1

*P<0.05 denotes comparison between sham and each period after SCI.
# P<0.05 denotes comparison of effects of apamin at each period.

Table 2. Summarized data of infusion volume and time to reach 30cmH_20.

	Infusion volume (μl)	Infusion time (min)
Sham (n=11)	298±53	11.9±2.0
1day (n=10)	432±95*	24.3±4.1*
2day (n=12)	568±105*	23.5±4.7*
3day (n=9)	539±78*	24.1±3.9*
14day (n=6)	905±126*	36.2±5.0*
30day (n=6)	1108±67*	41.2±2.6*

*P<0.05 denotes comparison between sham and each period after SCI.

Figures

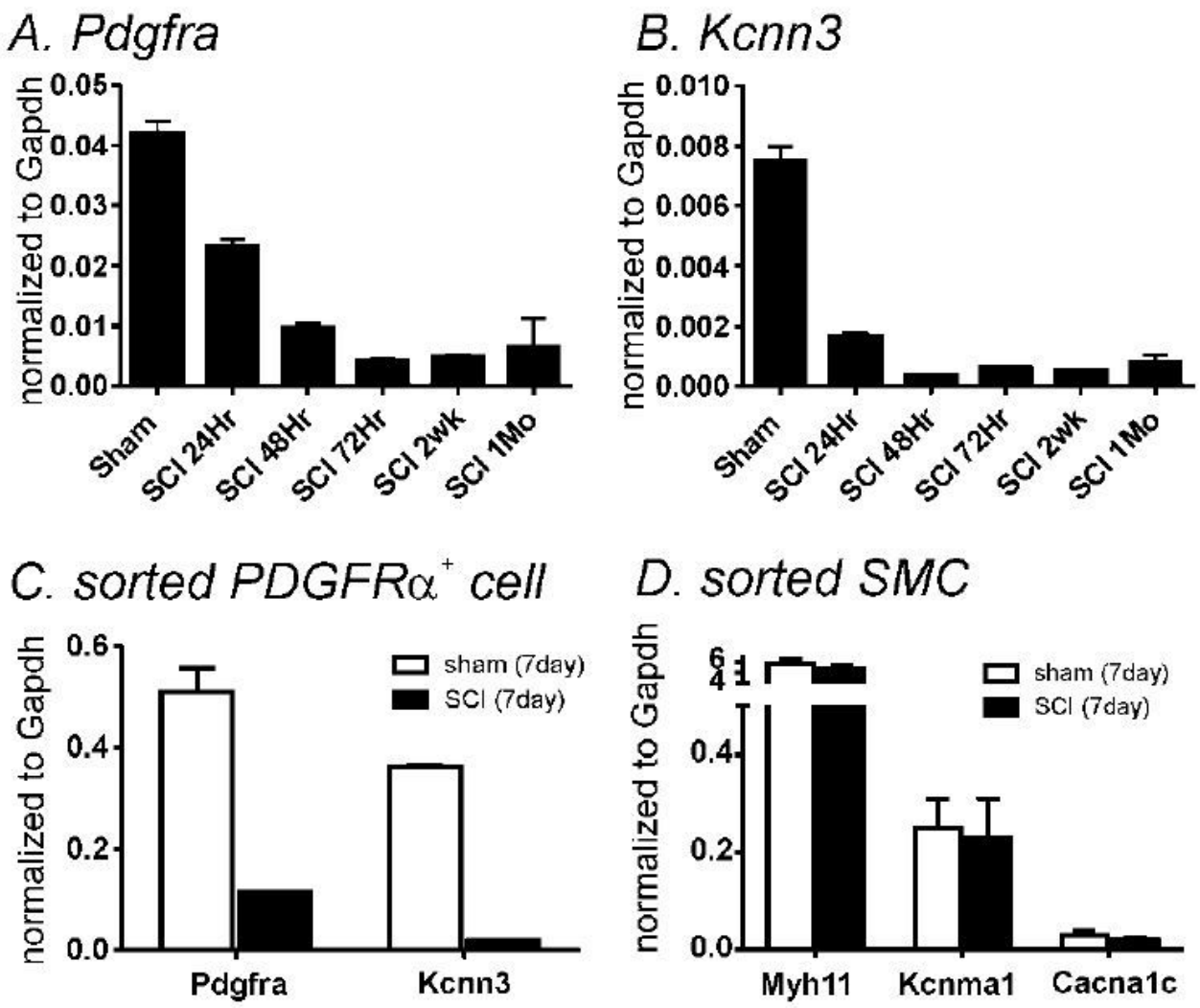

Figure 1

Quantitative analysis of transcripts in Sham and after SCI. A&B. Pdgfra and Kcnn3 transcripts are decreased up to 1month after SCI in detrusor muscles. C. Transcripts of Pdgfra and Kcnn3 from sorted PDGFRα+ cells in SCI (7day) decreased compared to sham (7day). D. Transcripts including Myh11, Kcnma1 and Cacna1C from sorted SMCs showed no significant change in SCI (7day). Error bars denote standard deviation from n=4.

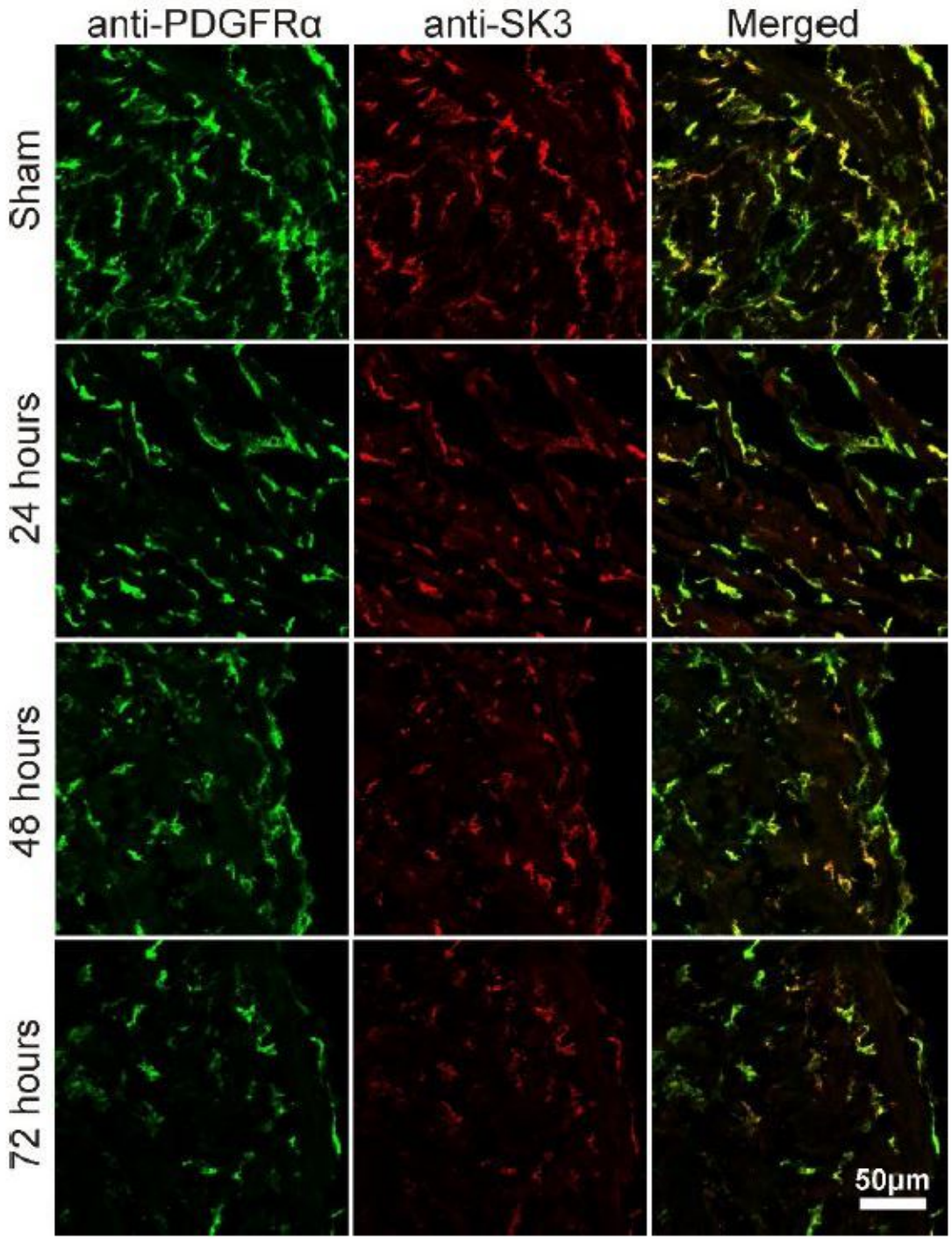

Figure 2

PDGFRα immunoreactivity of detrusor muscle layer in control and SCI. Immunoreactivity of PDGFRα (green) and SK3 (red) in control (sham). SCI (24hr, 48hr and 72 hr).

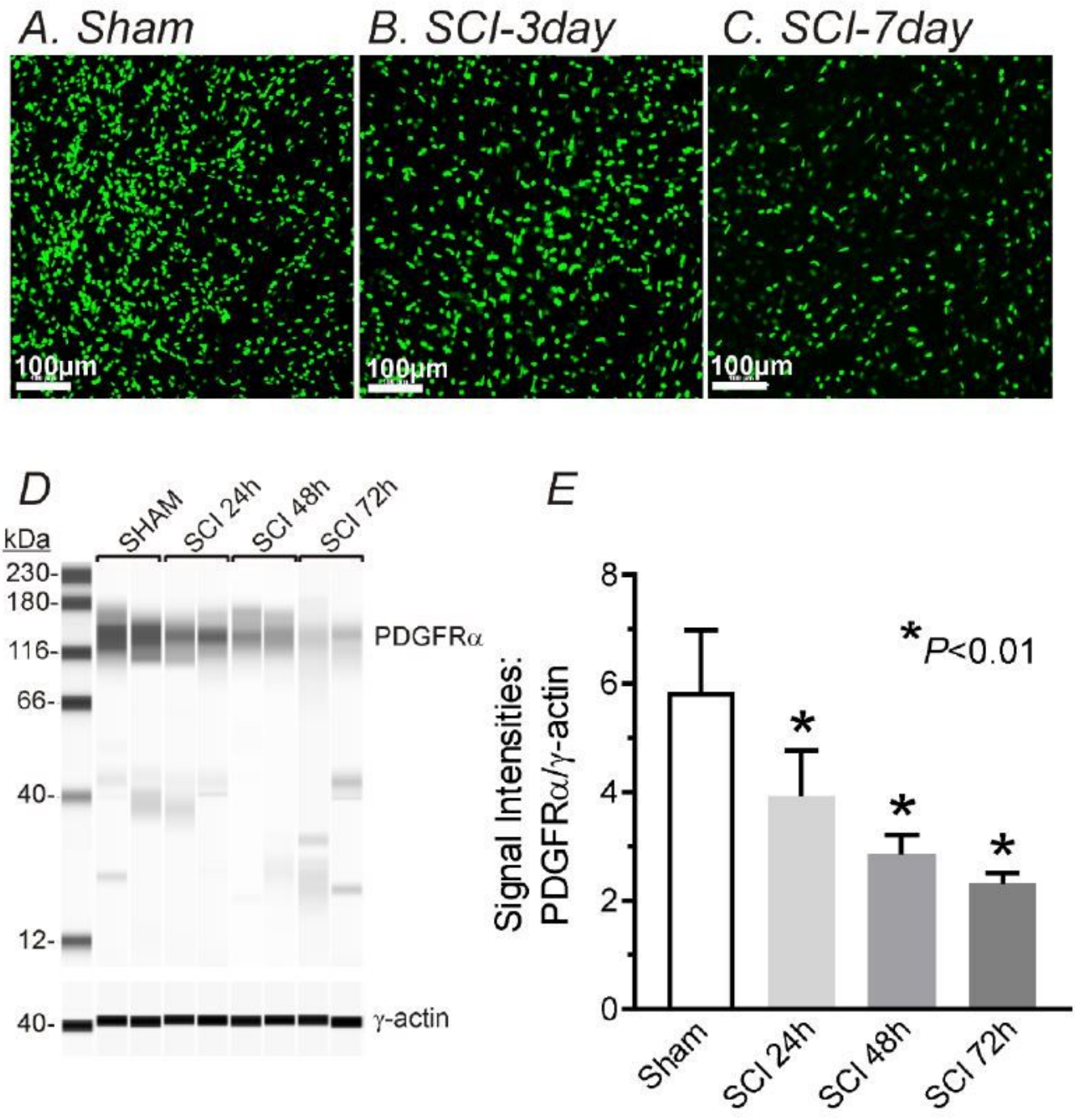

Figure 3

Density of PDFGRα/eGFP cells and Microcapillary electrophoresis and immunodetection of PDGFRα by WES in control and SCI detrusor muscles. A-C. Far fewer eGFP+ nuclei (reporter for PDGFRα+ cells) were found in detrusor muscles after SCI. D. Representative Wes full length gel image of PDGFRα expression in murine detrusor muscles following SCI. 100,000 x g pellet, 1μg/lane, γ-action was used for normalization. E. Normalized signal intensities of PDGFRα by g-actin following SCI periods.

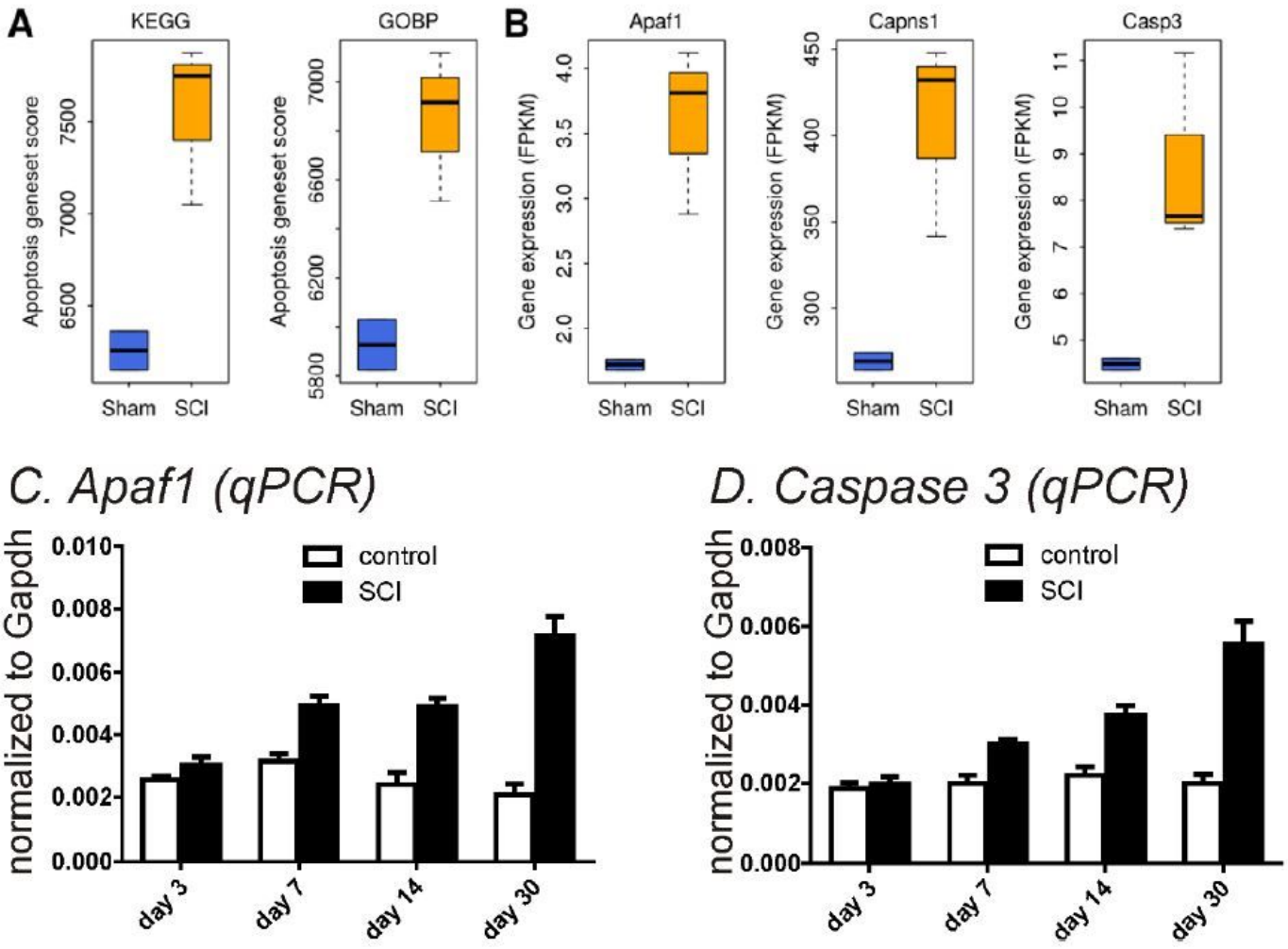

Figure 4

SCI -induced alteration in apoptosis-related genes by RNA-seq (A &B) and qPCR (C & D). A. Apoptosis geneset scores upregulated in SCI for both the KEGG and GOBP definitions. B. Expression of three apoptosis-related genes were upregulated in SCI. C & D. qPCR from sorted PDGFRα+ cells in SCI up to 30days showed an increase in apoptosis-related transcripts (Apaf1 in C and Caspase3 in D).

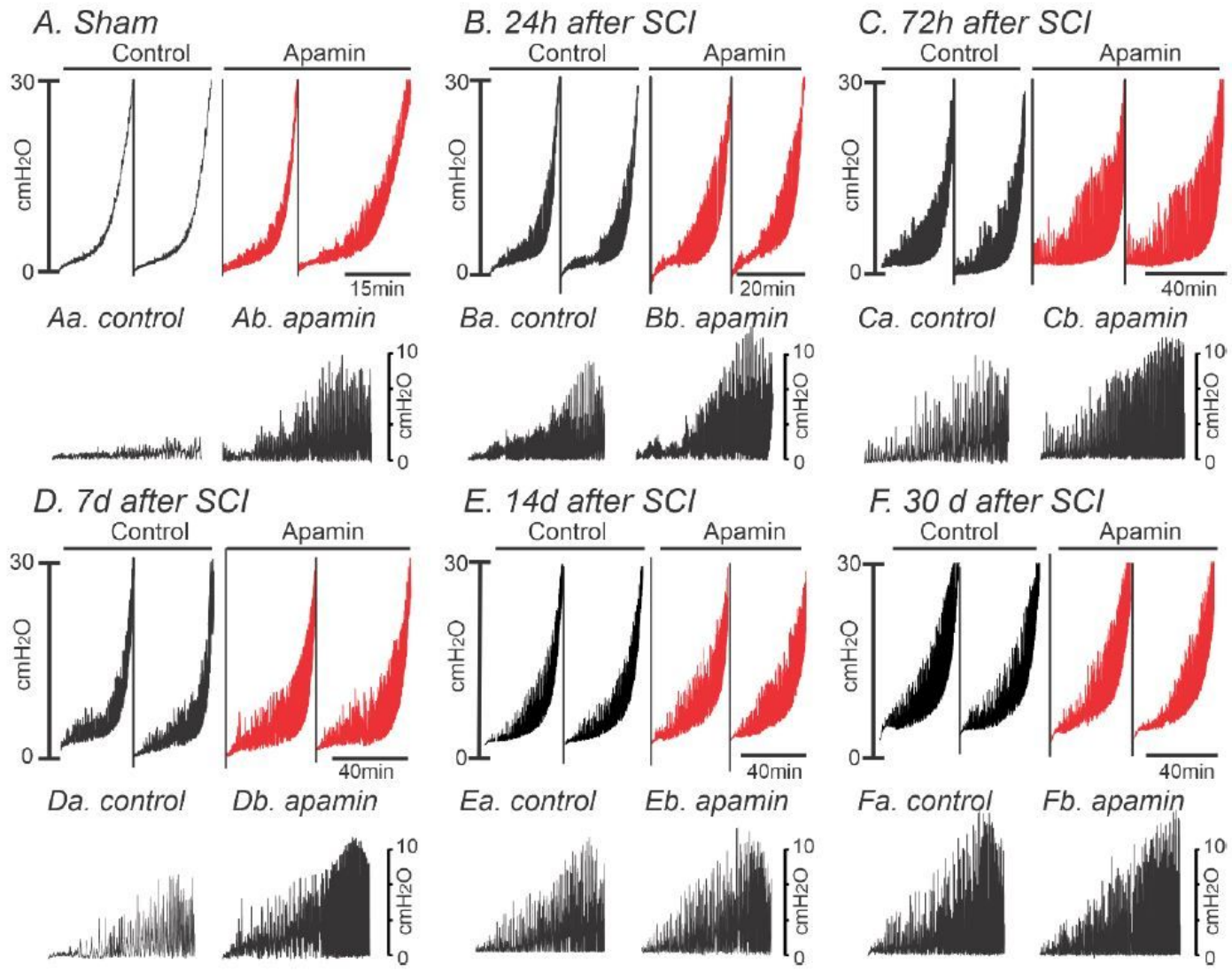

Figure 5

The effects of apamin on transient contractions (TCs) of sham, 1,3,7,14 and 30day after SCI using ex vivo preparation. A-F. Ex vivo pressure-response curve for control and apamin application. Aa,b-Fa,b. Expanded time scales with adjustment of baseline under control (a) and apamin (b) from above panels.